Water Science & Technology

IWA PUBLISHING

Water Science & Technology Vol 87 No 11, 2840 doi: 10.2166/wst.2023.150

Pharmacological assessment of Co_3O_4, CuO, NiO and ZnO nanoparticles via antibacterial, anti-biofilm and anti-quorum sensing activities

Bindia Junejo[a], Mujde Eryilmaz[b], Suna Sibel Rizvanoglu[b], Ismail Murat Palabiyik[c], Tania Ghumro[a], Arfana Mallah[d,e], Amber R. Solangi[a], Syed Iqleem Hyder[f], Hassan Karimi Maleh[g] and Elena Niculina Dragoi[h,*]

[a] National Centre of Excellence in Analytical Chemistry, University of Sindh Jamshoro, Sindh 76080, Pakistan
[b] Department of Pharmaceutical Microbiology, Faculty of Pharmacy, Ankara University, Ankara 06100, Turkey
[c] Department of Analytical Chemistry, Faculty of Pharmacy, Ankara University, Ankara 06100, Turkey
[d] Department of Chemistry, Norwegian University of Science and Technology (NTNU), Trondheim 7491, Norway
[e] M. A. Kazi Institute of Chemistry, University of Sindh, Jamshoro 76080, Pakistan
[f] Department of Chemistry, Government College University, Hyderabad, Sindh, Pakistan
[g] School of Resources and Environment, University of Electronic Science and Technology of China, P.O. Box 611731, Xiyuan Ave., Chengdu, China
[h] Cristofor Simionescu" Faculty of Chemical Engineering and Environmental Protection, 'Gheorghe Asachi' Technical University, Bld D. Mangeron no. 73, Iasi 700050, Romania
*Corresponding author. E-mail: elenan.dragoi@gmail.com

END, 0000-0001-5006-000X

ABSTRACT

Infectious diseases have risen dramatically as a result of the resistance of many common antibiotics. Nanotechnology provides a new avenue of investigation for the development of antimicrobial agents that effectively combat infection. The combined effects of metal-based nanoparticles (NPs) are known to have intense antibacterial activities. However, a comprehensive analysis of some NPs regarding these activities is still unavailable. This study uses the aqueous chemical growth method to synthesize Co_3O_4, CuO, NiO and ZnO NPs. The prepared materials were characterized by scanning electron microscopy, transmission electron microscopy and X-ray diffraction techniques. The antibacterial activities of NPs were tested against Gram-positive and Gram-negative bacteria using the microdilution method, such as the minimum inhibitory concentration (MIC) method. The best MIC value among all the metal oxide NPs was 0.63 against *Staphylococcus epidermidis* ATCC12228 through ZnO NPs. The other metal oxide NPs also showed satisfactory MIC values against different test bacteria. In addition, the biofilm inhibition and antiquorum sensing activities of NPs were also examined. The present study presents a novel approach for the relative analysis of metal-based NPs in antimicrobial studies, demonstrating their potential for bacteria removal from water and wastewater.

Key words: antibacterial activity, antiquorum sensing, biofilm inhibition, metal oxide nanoparticles

HIGHLIGHTS

- Metal oxide nanoparticles were synthesized using the chemical growth method.
- The prepared materials were characterized by scanning electron microscopy, transmission electron microscopy and X-ray diffraction techniques.
- The antimicrobial activity was tested against Gram-positive and Gram-negative bacteria.

GRAPHICAL ABSTRACT

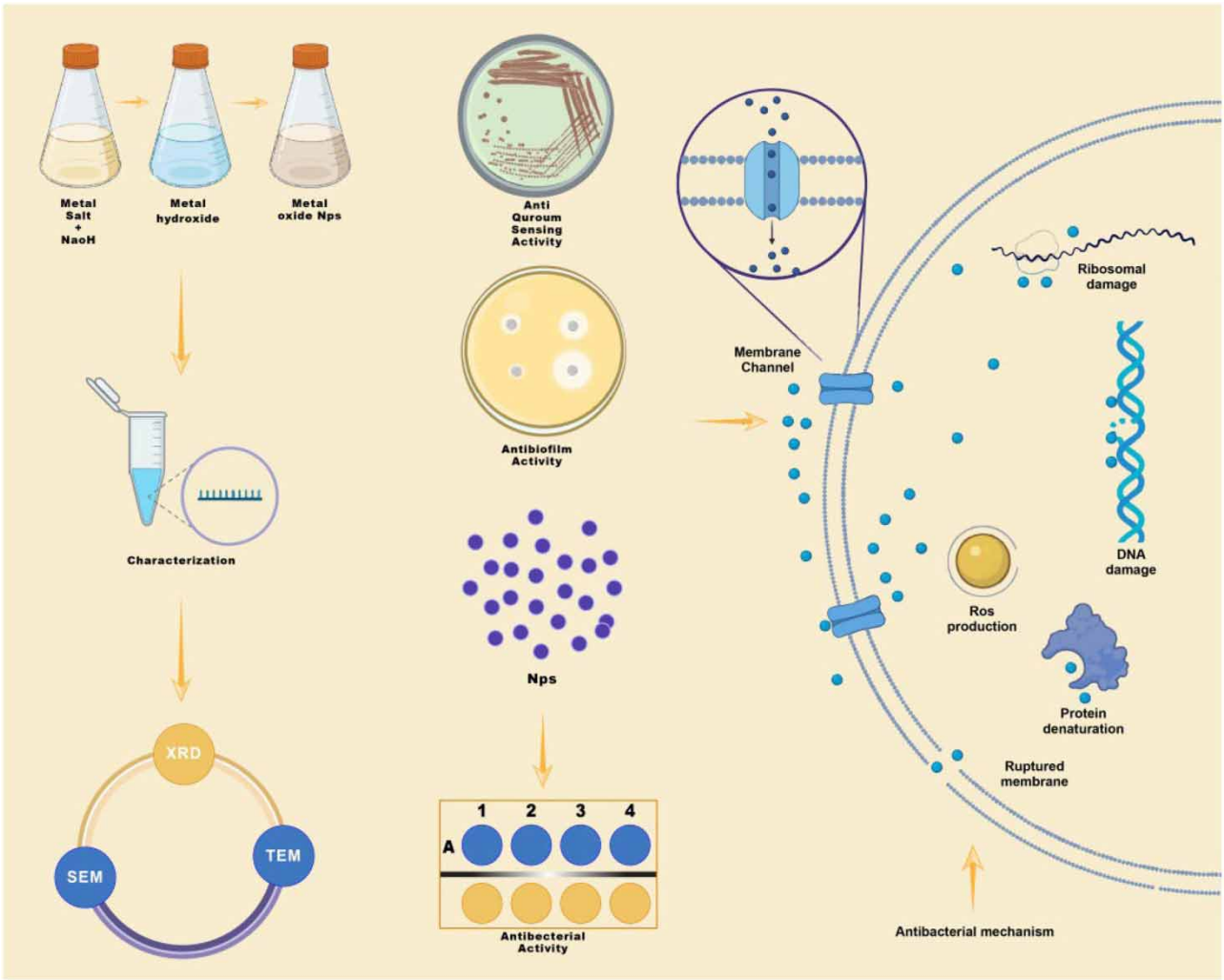

INTRODUCTION

Mortality and illness are on the rise throughout the world today. The infectious diseases brought on by antibiotic-resistant bacteria represent one of the causes of this increase. Reports of new antibiotic-resistant bacterial species emerge daily from all corners of the globe, and as a result, new strategies for protecting against them are sought. Unfortunately, in the latest years, scientists had little success in discovering new antibiotic groups to treat these harmful microorganisms (Islam *et al.* 2017; World Health Organization 2017; Bhatia 2018).

Antibiotic resistance

Antibiotics currently play a crucial role in the treatment of bacterial diseases. However, antibiotic resistance is recognized as a significant problem because some microorganisms have developed resistance to multiple drugs (Gudkov *et al.* 2021). Various mechanisms cause antibiotic resistance in bacteria, like the hindrance of drugs from entering the cell, inactivation of enzymes in antibiotics, alterations in antibiotic targets and so on (Kumar & Schweizer 2005; Alekshun & Levy 2007; Randall *et al.* 2013; Blair *et al.* 2014). Due to the severity of bacterial antibiotic resistance, there has been a significant rise in the number of deaths (Parks & Messmer 2015). There has also been a recent rise in the mortality rate of Covid-19 patients due to bacterial infections (Langford *et al.* 2020; Sharifipour *et al.* 2020). These factors have prompted scientists and researchers to search for effective antimicrobial agents to combat such a pervasive problem. Metal and metal oxide nanoparticles

(NPs) have recently been used as effective antibacterial agents against pathogenic and multidrug-resistant bacteria (Khan 2018; Tunio *et al.* 2020).

Interaction of metal oxide NPs with bacterial cells

The advanced developments in nanomaterial science and technology enable researches to improve in various application areas such as environmental remediation and treatment (Aboli *et al.* 2020; Ameen *et al.* 2021; Bae & Hong 2021), catalyst (Lee *et al.* 2021; Dhiman *et al.* 2022; Megarajan *et al.* 2022), biotechnology (Fathy & Mahfouz 2021; Ameen *et al.* 2023a; Begum *et al.* 2022), energy (Hosseinzadeh *et al.* 2021; Karimi-Maleh *et al.* 2022a), food analysis, sensor (Hussain *et al.* 2022; Gorle *et al.* 2022; Karimi-Maleh *et al.* 2022b; Ameen *et al.* 2023b; Zhang & Karimi-Maleh 2023a, 2023b), and optics (Yu *et al.* 2020). The NPs are materials with a small size of 100 nm or less. The properties of many standard materials can be changed when they are transformed into NPs (Singh *et al.* 2012). The large surface area of NPs enables more interaction with the bacterial cell walls. Metal oxide NPs are found to be selective, durable and resistant to heat and therefore could be excellent antimicrobial agents. They have minimum effects on human cells while simultaneously having toxic effects on bacterial cells (Fu *et al.* 2005; Reddy *et al.* 2007). There are numerous ways to kill bacteria with NPs, including binding with the enzymes inside the cells, generating reactive oxygen species (ROS), deactivating them, and directly destroying the cell wall. The bactericidal activity of metal oxide NPs depends on several factors, such as concentration, size and stability. Specific interactions with NPs can inhibit bacterial growth. Usually, the bacterial cell has a micrometer scale size while the cell membrane has nanometer pores. The NPs are smaller than bacterial pores and can easily pass through the membrane and generate ROS. However, it is challenging to synthesize stable NPs that can function effectively within the medium in which bacteria grow (Azam *et al.* 2012a).

Antibacterial properties of metal oxide NPs

The use of NPs is of much interest nowadays, and many metals and metal oxide NPs are found toxic to bacteria and are used as antimicrobial coatings. Examples include zinc oxide (ZnO), copper oxide (CuO), magnesium oxide (MgO) and titanium oxide (TiO_2) (Singh *et al.* 2012). The ZnO NPs have photo-oxidizing properties against many biological and chemical species. These NPs have been reported as the best antifungal and antibacterial agents when coated on different products like textile materials (Abramov *et al.* 2009). Zinc is an essential element, and ZnO NPs are reported as non-toxic for human cells' DNA. İn a study by Yamamoto (2001), ZnO NPs exhibit the best antimicrobial properties in different particle sizes ranging from 10 to 50 nm.

CuO NPs are also known as good antibacterial agents in different forms. The soluble compounds of Cu have been reported to show excellent antimicrobial activity against several microorganisms like fungi, bacteria, viruses and algae (Grass *et al.* 2011). The killing effect of CuO NPs for the microbes is either by generating ROS, which can cause irrecoverable damage like the cleavage of RNA and DNA and lipid peroxidation, which is subjected to membrane damage or the oxidation of enzymes (Halliwell & Gutteridge 1984; Pena *et al.* 1998).

The antibacterial activities of Co_3O_4 NPs are also studied extensively (Koyyati *et al.* 2016; Raza *et al.* 2016; Igwe & Ekebo 2018; Shahzadi *et al.* 2019; Kharade Suvarta *et al.* 2020). The Co_3O_4 NPs are excellent antibacterial agents for treating many infections caused by bacteria like *Klebsiella pneumoniae*, *Escherichia coli*, *Streptococcus pyrogens* and *Staphylococcus aureus* (Igwe & Ekebo 2018). In addition, research showed that green synthesized Co_3O_4 NPs also successfully inhibit the bacteria (Koyyati *et al.* 2016).

The NiO NPs were tested against the inhibition of Gram-positive and Gram-negative bacteria (Behera *et al.* 2019). The mechanism of the interaction of NiO NPs was based on the amount of ROS generated at the surface of NiO NPs. The excellent antibacterial and antiquorum sensing activity of NiO NPs was studied against *P. aeruginosa* and *Artemia franciscana* (Behera *et al.* 2019). The results showed that NiO NPs possess great potential to fight against these bacteria. The degradation of ring biofilm confirmed the biofilm inhibition and time-kill variation assays (Maruthupandy *et al.* 2020).

Quorum sensing is an effective tool in determining pathogenicity and biofilm formation. However, a particular focus was given to antibiofilm and antiquorum sensing studies, which are also used as alternatives for treating infections caused by bacteria (Uroz *et al.* 2009; Nithya *et al.* 2010).

Metal oxide NPs have several physicochemical properties that enable them to serve as effective antimicrobial agents instead of conventional antibiotic drugs, which typically have many side effects. This study aims to synthesize Co_3O_4, CuO, NiO and ZnO NPs and to check their antimicrobial activities through disc diffusion, well diffusion and minimum

inhibitory concentration (MIC) methods. Their antiquorum sensing and antibiofilm activities are checked against *Chromobacterium violaceum* ATCC 12472 and *Pseudomonas aeruginosa* PAO1 bacteria.

MATERIALS AND METHODS

Synthesis of metal oxide NPs

Metal oxide NPs were synthesized using the aqueous chemical growth method in which the metal salt and sodium hydroxide were used in a 1:2 ratio in double distilled water. The mixture was stirred for about 30 min at 25 °C, then placed in a Fotile oven at 90 °C for 4 h, and filtered. The filtrate was dried further in the oven at 60 °C for 1 h; the pure metal hydroxide material was obtained (Bakhsh *et al.* 2021). Finally, the material was calcinated using a muffle furnace at 500 °C for 4 h. The pure metal oxide material obtained was further characterized using X-ray diffraction (XRD), scanning electron microscopy (SEM) and transmission electron microscopy (TEM) analysis.

Characterization of metal oxide NPs

The SEM analysis was done for all the synthesized materials using the 30 KV Scanning Electron Microscope (JSM5910, Jeol, Japan) with secondary electron imaging (SEI) and energy dispersive X-ray (EDX) detectors (INCA200/Oxford Instruments, UK). The synthesized NPs were also characterized using TEM as a 200 KV Transmission Electron Microscope (JM 2100, Jeol, Japan) with EDX (INCA100/ Oxford Instruments, UK). XRD analysis for the synthesized NPs was carried out using the X-ray Diffractometer (JDX 3532, Jeol, Japan) with CuKα source.

Antibacterial activity tests

The microdilution method was used to determine the antibacterial activities of the metal oxide NPs (Co_3O_4, CuO, NiO and ZnO). The prepared NPs were dissolved in dimethyl-sulfoxide (10% DMSO).

MIC method

In the antibacterial activity tests, *S. aureus* ATCC 25923, methicillin-resistant *S. aureus* ATCC 43300 (MRSA), *Staphylococcus epidermidis* ATCC 12228, *Enterococcus faecalis* ATCC 29212, *Bacillus subtilis* ATCC 6633, *Escherichia coli* ATCC 25922, *K. pneumoniae* ATCC 13883, *P. aeruginosa* ATCC 27853 were used as test bacteria. The broth microdilution method was used to determine MIC values (Wikler 2006). Two-fold dilutions ranging from 10 to 0.08 mg/mL were prepared in Mueller Hinton Broth (Difco, Difco Laboratories, Detroit, MI, USA). The inoculums were prepared from subcultures for 24 h. The final test concentration of the bacteria was adjusted to 5×10^5 CFU/mL. The microplates were incubated at 35 °C for 18–24 h. The last well that completely inhibited visual microbial growth was noted as the MIC value (mg/mL). A set of wells containing only inoculated broth and 10% DMSO were used as the negative control. Ampicillin (Sigma, USA), ciprofloxacin (Sigma, USA), and ofloxacin (Sigma, USA) were used as reference drugs.

Antibiofilm activity test

The antibiofilm activity was determined by the *in vitro* microplate-based biofilm model against *P. aeruginosa* PAO1 using the crystal violet assay (Bali *et al.* 2019; Eryılmaz *et al.* 2019; Jardak *et al.* 2021).

Biofilm formation. *P. aeruginosa* PAO1 was incubated for 24 h at 37 °C in Brain Heart Infusion (BHI) broth. After incubation, final inoculum suspensions containing ~10^6 CFU/mL of *P. aeruginosa* were prepared in BHI enriched with 2% sucrose. Next, 100 µL of the inoculum suspensions were added to 96-well microtiter plates for each test condition. Then, the plates were incubated at 37 °C for 72 h to form mature biofilms.

Treating the biofilm cells with the extracts. Following biofilm formation, the medium was aspirated, and no adhered cells were removed by washing the wells with sterile phosphate-buffered saline (PBS, pH 7.2). The solutions of metal oxide NPs (ZnO, CuO, Co_3O_4 and NiO) were transferred into mature *P. aeruginosa* biofilms wells. The plates were incubated at 37 °C for 24 h. After incubation, the content of the wells was poured off, and the wells were washed with PBS. The plates were then dried at room temperature for 1 h. Next, 100 µL of 0.5% crystal violet solution was added to each well for staining the biofilm cells. After 30 min, the wells were washed three times with PBS. Then acetone–alcohol (30:70 v/v) solution was added into the wells to dissolve the bound dye within the biofilm matrix. BHI broth enriched with 2% sucrose and 10% DMSO was used as negative controls. The optical density of the dissolved crystal violet dye was

measured by a microplate reader (Thermo Scientific Multiskan GO Microplate Spectrophotometer, Vantaa, Finland) at 620 nm (OD 620nm). The percentage biofilm inhibition values were calculated according to the following formula:

$$\%\ \text{biofilm inhibition} = [(\text{OD(growth control)} - \text{OD(sample)})/\text{OD(growth control)}] \times 100$$

Antiquorum sensing activity test

The antiquorum sensing activity was performed by the disc diffusion method using the reported bacteria *C. violaceum* ATCC 12472 (Gajdács & Spengler 2019; Batohi *et al.* 2021). The density of the overnight bacterial culture was adjusted to 1.5×10^8 CFU/mL. Then the bacterial suspension was inoculated on Luria Bertani Agar. The sterile blank discs (6 mm diameter; Bioanalyse®, Ankara, Turkey) impregnated with 20 µL of the metal oxide NPs (ZnO, CuO, Co_3O_4 and NiO) solutions were placed on the medium. After incubation at 30 °C for 24 h, the plates were observed for a zone of violacein inhibition. The formation of an inhibition zone around the discs was noted as the potential antiquorum sensing activity.

RESULTS

Characterization results of metal oxide NPs

SEM analysis

The SEM images of Co_3O_4, CuO, NiO and ZnO NPs are shown in Figure 1. Figure 1(a) shows the spherical shape of Co_3O_4 NPs. The porous structure of NPs is due to the magnetic nature of the material (Memon *et al.* 2020). Figure 1(b) shows the nanorod-like structure of CuO NPs, which is in good agreement with the literature (Lanje *et al.* 2010). The cluster-shaped NiO NPs (Zorkipli *et al.* 2016) are shown in Figure 1(c), while Figure 1(d) shows the spherical and agglomerated structure of ZnO NPs (Ghimire *et al.* 2022). The surface of metal oxide NPs shown here looks agglomerated, which may be due to the adhesion of particles to each other by weak forces leading to (sub)micron-sized entities. The morphology of NPs indicates well-uniform particles with narrow size distribution in the range of 10–95 nm. The surface of synthesized NPs is very smooth, facilitating better contact with the bacteria.

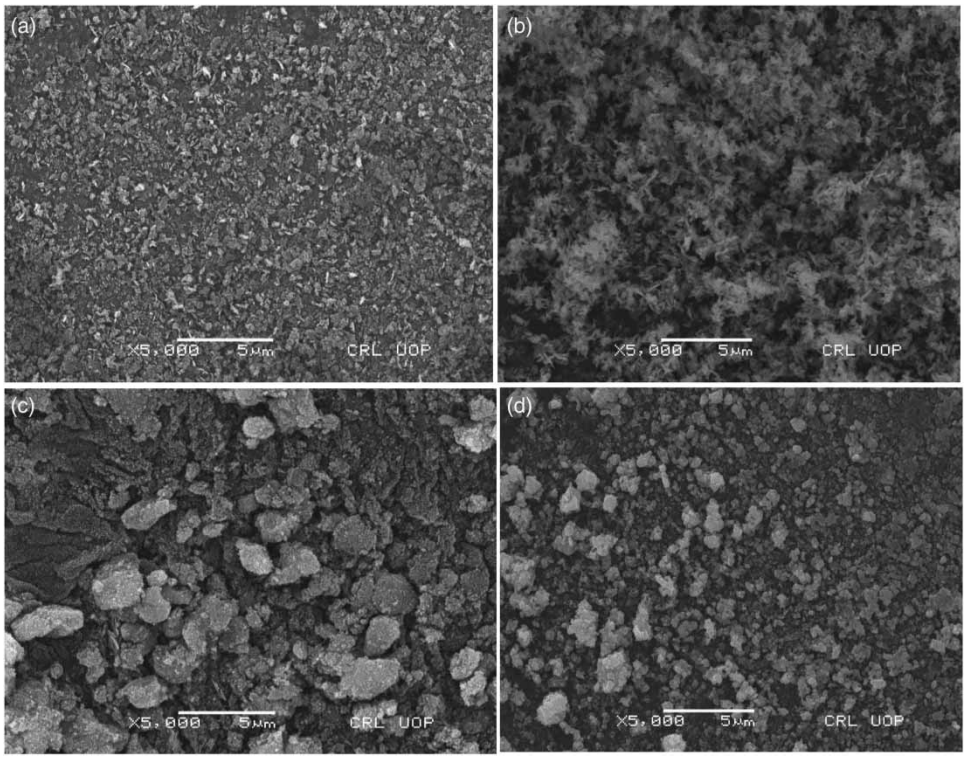

Figure 1 | SEM images of (a) Co_3O_4 NPs, (b) CuO NPs, (c) NiO NPs and (d) ZnO NPs.

TEM analysis

TEM is used to determine the size and morphology of NPs. Figure 2(a)–2(c) and 2(d) shows the TEM images of synthesized Co_3O_4, CuO, NiO and ZnO NPs, whereas Figure 2(e)–2(g) and 2(h) shows the size calculation of these NPs with Image J software. Figure 2(a) shows the hexagonal and crystal-like shape of Co_3O_4 NPs, and the size of NPs is calculated using the image J software. The Co_3O_4 NPs are 50–98 nm in size (Figure 2(e)) (Das & Saikia 2023). Figure 2(b) shows the agglomerated and clustered shape of CuO NPs with an average size of 80–99 nm (Figure 2(f)). Similar results were found in the literature (Lanje *et al.* 2010).

The NiO NPs shown in Figure 2(c) appear as nanorods with a 20–25 nm size (Figure 2(g)) range comparable to the TEM image of NiO NPs reported in Sagadevan & Podder (2015). Figure 2(d) shows the spherical shape of ZnO NPs with a calculated size range of 70–95 nm (Figure 2(h)) (Akpomie *et al.* 2021).

X-ray diffraction

Figure 3 shows the XRD pattern of the prepared metal oxide NPs. The XRD peaks red, orange, green and blue represent the characteristic patterns of Co_3O_4, CuO, NiO and ZnO. The crystalline nature and phase purity of Co_3O_4 NPs have been studied through XRD. The diffraction peaks at (111), (240), (311), (400), (511) and (400) are highly sharp, which correspond to the highly crystalline and cubic phase structure of Co_3O_4 NPs. However, the absence of other peaks shows no impurities in the synthesized material. The XRD peaks are in good agreement with the literature (Khand *et al.* 2021).

The diffraction peaks of CuO at (002), (111), (202), (113) and (220) show the monoclinic phase of the synthesized CuO NPs, while no unwanted or extra peaks appear in the XRD pattern as an impurity can be observed (Buledi *et al.* 2020). The XRD pattern of NiO with highly sharpened peaks at (111), (200), (220), (311) and (222) confirms the pure and crystalline phase structure of NiO NPs, which is comparable with the reported XRD peaks of NiO NPs (Sagadevan & Podder 2015) ZnO has XRD diffraction peaks at (002), (102) and (112) and highly sharp peaks at (100), (101), (110) and (103), which shows the hexagonal crystalline nature of the synthesized ZnO NPs (Ghimire *et al.* 2022). The average crystalline size of all synthesized NPs was calculated from the major XRD peaks using the Scherer formula ($\tau = k\lambda/(\beta \cos \theta)$), and the average size for Co_3O_4, CuO, NiO and ZnO was found to be 80.4, 90.1, 18.4 and 94.1, respectively.

Antibacterial tests

The results for the MIC of NPs against test bacteria are given in Table 1.

Several microbial species' growth was inhibited at various concentrations, as determined by the MIC test results. The low MIC value indicates that the material used as an antibacterial agent possesses effective antibacterial activity. The current work studied the low MIC value against Gram-positive bacterial species, i.e. *S. epidermidis* ATCC 12228 for ZnO NPs, at 0.63 mg/mL. The excellent antibacterial activity of ZnO NPs is due to the generation of ROS from the ZnO NPs surface, causing oxidative stress and damaging the cell DNA and proteins. The contact between NPs and bacterial cell causes toxic effects for the bacterial species. Zn^{2+} ions are released due to such contact, causing damage to the whole intracellular area (Klink *et al.* 2022).

In contrast, the positive controls ampicillin, ciprofloxacin and ofloxacin showed no activity against this tested bacteria. The MIC value of CuO NPs was found as 1.25 for the Gram-positive bacteria, i.e. *Staphylococcus* ATC12228 and *E. faecalis* ATCC 29212, while the drug ciprofloxacin showed a better MIC (0.0625) in the case of *E. faecalis*. Co_3O_4 NPs show a good MIC (1.25) in the case of *E. faecalis* ATCC 29212. Ciprofloxacin obtains a minimal MIC (0.0625) against *K. pneumoniae*, compared to CuO and ZnO NPs, which show MIC at values 2.5 and 5. The reason for such variation in MIC values may be attributed to factors such as differences in physiology and cell structure or the degree of contact of these bacterial species with the NPs. Another reason may be the NPs diffusion rate, affecting their ability to resist such microbial organisms (Azam *et al.* 2012b).

Antibiofilm activity

The percentage of biofilm inhibition can be seen in Figure 4 for the synthesized metal oxide NPs. The percent inhibition of NiO is 88.5%, which is better than the other NPs. The CuO NPs show inhibition at 85.95%, while the Co_3O_4 and ZnO NPs are at 80.35 and 83.99%, respectively. The interaction between NPS and biofilms can be illustrated by electrostatic features, depending mainly on the charge of the biofilm matrix. Most of the bacteria have polyionic biofilm matrix with carboxylic acid functions. The positively charged metallic NPs usually interact with the negatively charged biofilm matrix by electrostatic

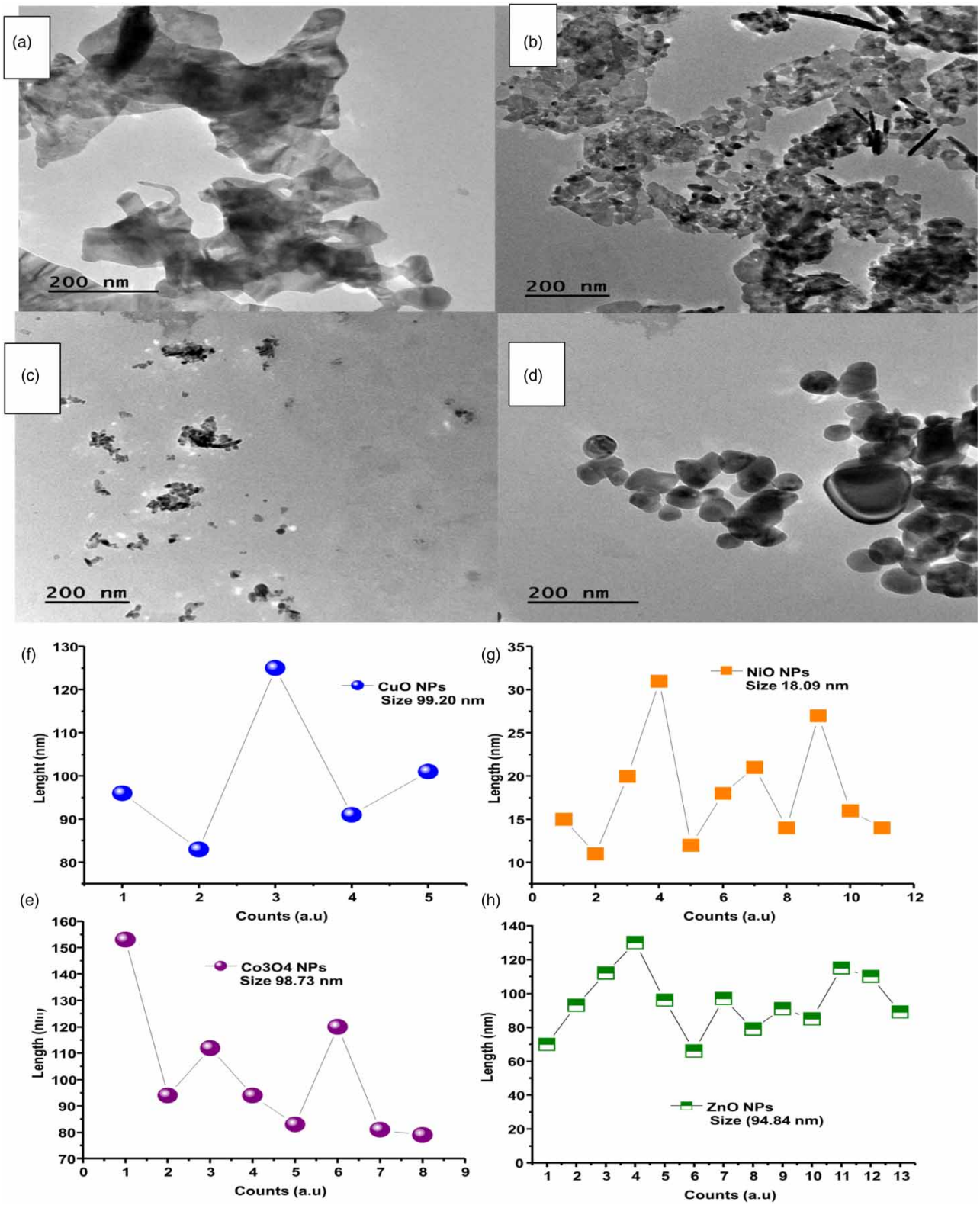

Figure 2 | TEM images of (a) Co_3O_4 NPs, (b) CuO NPs, (c) NiO NPs, (d) ZnO NPs, (e) Image J picture of Co_3O_4 NPs, (f) Image J picture of CuO NPs, (g) Image J picture of NiO NPs and (h) Image J picture of ZnO NPs.

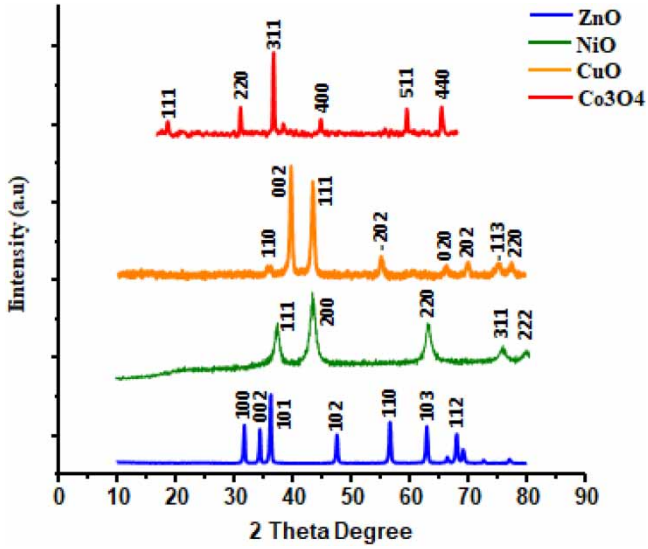

Figure 3 | XRD spectra of Co_3O_4, CuO, NiO and ZnO.

Table 1 | MIC values (mg/mL) of metal oxide NPs against tested bacteria

Test bacteria		NiO	Co_3O_4	CuO	ZnO	Ampicillin	Ciprofloxacin	Ofloxacin	DMSO (10%)
Gram-positive	*S. aureus* ATCC 25923	–	5	5	5	0.0016	NT	NT	–
	S. aureus ATCC 43300 (MRSA)	–	5	2.5	5	0.05	NT	NT	–
	S. epidermidis ATCC 12228	10	–	1.25	0.63	–	–	–	–
	E. faecalis ATCC 29212	10	1.25	1.25	10	NT	0.0625	NT	–
	B. subtilis ATCC 6633	5	5	2.5	5	–	–	–	–
Gram-negative	*E. coli* ATCC 25922	–	–	2.5	5	NT	NT	0.001	–
	K. pneumoniae ATCC 13883	–	–	2.5	5	NT	0.0625	NT	–
	P. aeruginosa ATCC 27853	–	–	–	–	NT	NT	0.008	–

'–' represents no activity.
NT, not tested.

forces. In some cases, the size of NPs is also crucial in determining the penetration of NPs deep down the biofilm to resist bacterial growth. Despite these two main factors, there must be other possible ways of interaction between NPs and bacterial cells to be determined (Shkodenko *et al.* 2020).

Antiquorum sensing activity

The formation of a transparent inhibition zone around the disc indicates the potential QS inhibitory activity. None of the tested metal oxide NPs showed antiquorum sensing activity (Figure 5). This may be because the testing sample's killing capacity is below the minimum required concentration. Hence, contact between NPs and the bacterial cell wall is sufficient to cause toxicity; therefore, large amounts of metal NPs are required to completely envelop bacterial cells and shield them from the environment, leaving no chance for nutrition to be absorbed to continue the life process. The primary role of NPs here is to envelop the bacterial cells completely and shield them from the environment, leaving no space for their

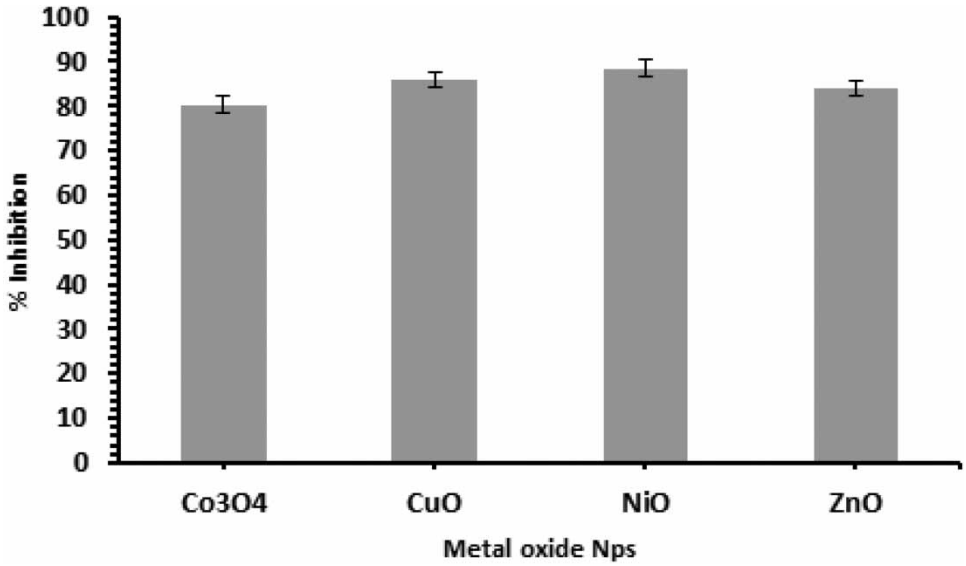

Figure 4 | Antibiofilm activities of metal oxide NPs.

Figure 5 | QS inhibitory activity of the metal oxide NPs (1: Co_3O_4, 2: CuO 3: NiO, 4: ZnO).

growth and nutrition to continue their life process (Saleh *et al.* 2019; Theodora *et al.* 2019). Another explanation for the lack of antiquorum sensing activity is that the diffusion rate of NPs may not be enough to contact the bacterial cell wall.

CONCLUSION

This study explored the antibacterial properties of some selected metal oxide NPs. In this regard, metal oxide NPs (Co_3O_4, CuO, NiO and ZnO) are successfully synthesized and characterized using SEM, TEM and XRD. The average size of these prepared NPs was 10–20 nm, as calculated using TEM and XRD. The antibacterial activities of all the synthesized NPs

were studied by the MIC method. The ZnO showed its best MIC value at 0.63 against *S. epidermidis* ATCC 12228. The CuO, NiO and Co_3O_4 NPs showed satisfactory MIC values at 1.25 against *Enterococcus faecalis* ATCC 29212. The biofilm inhibition was also studied using these metal oxide NPs in which *P. aeruginosa* PAO1 was used as test bacteria. The antibiofilm activity of NPs was 88.5, 85.95, 80.35 and 83.99% for the NiO, CuO, Co_3O_4 and ZnO NPs, respectively. No results were observed in the case of antiquorum sensing activity tests. The reason may be the low diffusion rate of our synthesized materials into the media. The findings show that these metal oxide NPs can work as potential antibacterial agents in various biological applications.

DATA AVAILABILITY STATEMENT

All relevant data are included in the paper or its Supplementary Information.

CONFLICT OF INTEREST

The authors declare there is no conflict.

REFERENCES

Aboli, E., Jafari, D. & Esmaeili, H. 2020 Heavy metal ions (lead, cobalt, and nickel) biosorption from aqueous solution onto activated carbon prepared from Citrus limetta leaves. *Carbon Letters* **30** (6), 683–698.

Abramov, O., Gedanken, A., Koltypin, Y., Perkas, N., Perelshtein, I., Joyce, E. & Mason, T. J. 2009 Pilot scale sonochemical coating of nanoparticles onto textiles to produce biocidal fabrics. *Surface and coatings Technology* **204** (5), 718–722.

Akpomie, K. G., Ghosh, S., Gryzenhout, M. & Conradie, J. 2021 One-pot synthesis of zinc oxide nanoparticles via chemical precipitation for bromophenol blue adsorption and the antifungal activity against filamentous fungi. *Scientific reports* **11** (1), **8305**.

Alekshun, M. N. & Levy, S. B. 2007 Molecular mechanisms of antibacterial multidrug resistance. *Cell* **128** (6), 1037–1050.

Ameen, F., Al-Maary, K. S., Almansob, A. & AlNadhari, S. 2023a Antioxidant, antibacterial and anticancer efficacy of Alternaria chlamydospora-mediated gold nanoparticles. *Applied Nanoscience* **13**, 2233–2240.

Ameen, F., Dawoud, T. & AlNadhari, S. 2021 Ecofriendly and low-cost synthesis of ZnO nanoparticles from Acremonium potronii for the photocatalytic degradation of azo dyes. *Environmental Research* **202**, 1–7.

Ameen, F., Hamidian, Y., Mostafazadeh, R., Darabi, R., Erk, N., Islam, M. A. & Orfali, R. 2023b A novel atropine electrochemical sensor based on silver nano particle-coated Spirulina platensis multicellular blue-green microalga. *Chemosphere* **324**, 138180.

Azam, A., Ahmed, A. S., Oves, M., Khan, M. S., Habib, S. S. & Memic, A. 2012a Antimicrobial activity of metal oxide nanoparticles against Gram-positive and Gram-negative bacteria: A comparative study. *International journal of nanomedicine* **7**, 6003–6009.

Azam, A., Ahmed, A. S., Oves, M., Khan, M. & Memic, A. 2012b Size-dependent antimicrobial properties of CuO nanoparticles against Gram-positive and-negative bacterial strains. *International journal of nanomedicine* **7**, 3527–3535.

Bae, J. & Hong, J. Y. 2021 Fabrication of nitrogen-doped porous carbon nanofibers for heavy metal ions removal. *Carbon Letters* **31** (6), 1339–1347.

Bakhsh, H., Buledi, J. A., Khand, N. H., Junejo, B., Solangi, A. R., Mallah, A. & Sherazi, S. T. H. 2021 NiO nanostructures based functional none-enzymatic electrochemical sensor for ultrasensitive determination of endosulfan in vegetables. *Journal of Food Measurement and Characterization* **15**, 2695–2704.

Bali, E. B., Türkmen, K. E., Erdönmez, D. & Sağlam, N. 2019 Comparative study of inhibitory potential of dietary phytochemicals against quorum sensing activity of and biofilm formation by Chromobacterium violaceum 12472, and swimming and swarming behaviour of Pseudomonas aeruginosa PAO1. *Food technology and biotechnology* **57** (2), 212.

Batohi, N., Lone, S. A., Marimani, M., Wani, M. Y., Al-Bogami, A. S. & Ahmad, A. 2021 Citral and its derivatives inhibit quorum sensing and biofilm formation in Chromobacterium violaceum. *Archives of Microbiology* **203** (4), 1451–1459.

Begum, I., Shamim, S., Ameen, F., Hussain, Z., Bhat, S. A., Qadri, T. & Hussain, M. 2022 A Combinatorial Approach towards Antibacterial and Antioxidant Activity Using Tartaric Acid Capped Silver Nanoparticles. *Processes* **10** (4), **716**.

Behera, N., Arakha, M., Priyadarshinee, M., Pattanayak, B. S., Soren, S., Jha, S. & Mallick, B. C. 2019 Oxidative stress generated at nickel oxide nanoparticle interface results in bacterial membrane damage leading to cell death. *RSC advances* **9** (43), 24888–24894.

Bhatia, R. 2018 Universal health coverage framework to combat antimicrobial resistance. *The Indian journal of medical research* **147** (3), 228.

Blair, J. M., Richmond, G. E. & Piddock, L. J. 2014 Multidrug efflux pumps in Gram-negative bacteria and their role in antibiotic resistance. *Future microbiology* **9** (10), 1165–1177.

Buledi, J. A., Ameen, S., Khand, N. H., Solangi, A. R., Taqvi, I. H., Agheem, M. H. & Wajdan, Z. 2020 CuO nanostructures based electrochemical sensor for simultaneous determination of hydroquinone and ascorbic acid. *Electroanalysis* **32** (7), 1600–1607.

Das, D. & Saikia, B. J. 2023 Synthesis, characterization and biological applications of cobalt oxide (Co3O4) nanoparticles. *Chemical Physics Impact* **6**, 100137.

Dhiman, P., Goyal, D., Rana, G. & Kumar, A., Sharma G., Linxin and Kumar G. 2022 Recent advances on carbon-based nanomaterials supported single-atom photo-catalysts for waste water remediation. *Journal of Nanostructure in Chemistry*. https://doi.org/10.1007/s40097-022-00511-3.

Eryılmaz, M., Kart, D. & Gürpınar, S. S. 2019 Vajinal Floradan İzole Edilen Lactobacillus sp. *Metabolitlerinin Antibiyofilm Aktivitelerinin Araştırılması. Türk Mikrobiyoloji Cemiyeti Dergisi* **49** (3), 169–174.

Fathy, R. M. & Mahfouz, A. Y. 2021 Eco-friendly graphene oxide-based magnesium oxide nanocomposite synthesis using fungal fermented by-products and gamma rays for outstanding antimicrobial, antioxidant, and anticancer activities. *Journal of Nanostructure in Chemistry* **11** (2), 301–321.

Fu, L., Liu, Z., Liu, Y., Han, B., Hu, P., Cao, L. & Zhu, D. 2005 Beaded cobalt oxide nanoparticles along carbon nanotubes: Towards more highly integrated electronic devices. *Advanced Materials* **17** (2), 217–221.

Gajdács, M. & Spengler, G. 2019 Standard operating procedure (SOP) for disk diffusion-based quorum sensing inhibition assays. *Acta Pharmaceutica Hungarica* **89** (4), 117–125.

Ghimire, R. R., Parajuli, A., Gupta, S. K. & Rai, K. B. 2022 Synthesis of ZnO Nanoparticles by Chemical Method and its Structural and Optical Characterization. *BIBECHANA* **19** (1-2), 90–96.

Gorle, G., Bathinapatla, A., Kanchi, S., Ling, Y. C. & Rezakazemi, M. 2022 Low dimensional Bi2Se3 NPs/reduced graphene oxide nanocomposite for simultaneous detection of L-Dopa and acetaminophen in presence of ascorbic acid in biological samples and pharmaceuticals. *Journal of Nanostructure in Chemistry* **12** (4), 513–528.

Grass, G., Rensing, C. & Solioz, M. 2011 Metallic copper as an antimicrobial surface. *Applied and environmental microbiology* **77** (5), 1541–1547.

Gudkov, S. V., Burmistrov, D. E., Serov, D. A., Rebezov, M. B., Semenova, A. A. & Lisitsyn, A. B. 2021 A mini review of antibacterial properties of ZnO nanoparticles. *Frontiers in Physics* **9**, 641481.

Halliwell, B. & Gutteridge, J. 1984 Oxygen toxicity, oxygen radicals, transition metals and disease. *Biochemical journal* **219** (1), 1.

Hosseinzadeh, K., Moghaddam, M. A. E., Asadi, A., Mogharrebi, A. R., Jafari, B., Hasani, M. R. & Ganji, D. D. 2021 Effect of two different fins (longitudinal-tree like) and hybrid nano-particles (MoS2 - TiO2) on solidification process in triplex latent heat thermal energy storage system. *Alexandria Engineering Journal* **60** (1), 1967–1979.

Hussain, R. T., Islam, A. K. M. S., Khairuddean, M. & Suah, F. B. M. 2022 A polypyrrole/GO/ZnO nanocomposite modified pencil graphite electrode for the determination of andrographolide in aqueous samples. *Alexandria Engineering Journal* **61** (6), 4209–4218.

Igwe, O. & Ekebo, E. 2018 Biofabrication of cobalt Nanoparticle odorata and their potential. *Res J Chem* **8** (1), 11–17.

Islam, M. A., Islam, M., Hasan, R., Hossain, M. I., Nabi, A., Rahman, M., Goessens, W. H., Endtz, H. P., Boehm, A. B. & Faruque, S. M. 2017 Environmental spread of New Delhi metallo-β-lactamase-1-producing multidrug-resistant bacteria in Dhaka, Bangladesh. *Applied and environmental microbiology* **83** (15), e00793–00717.

Jardak, M., Mnif, S., Ayed, R. B., Rezgui, F. & Aifa, S. 2021 Chemical composition, antibiofilm activities of Tunisian spices essential oils and combinatorial effect against Staphylococcus epidermidis biofilm. *Lwt* **140**, 110691.

Karimi-Maleh, H., Karaman, C., Karaman, O., Karimi, F., Vasseghian, Y., Fu, L., Baghayeri, M., Rouhi, J., Kumar, P. S., Show, P. L., Rajendran, S., Sanati, A. L. & Mirabi, A. 2022a Nanochemistry approach for the fabrication of Fe and N co-decorated biomass-derived activated carbon frameworks: A promising oxygen reduction reaction electrocatalyst in neutral media. *Journal of Nanostructure in Chemistry* **12** (3), 429–439.

Karimi-Maleh, H., Darabi, R., Karimi, F., Karaman, C., Shahidi, S. A., Zare, N., Baghayeri, M., Fu, L., Rostamnia, S., Rouhi, J. & Rajendran, S. 2022b State-of-art advances on removal, degradation and electrochemical monitoring of 4-aminophenol pollutants in real samples: A review. *Environmental Research* **222**, 115338.

Khan, T. M. 2018 Synthesis of Cu Nanoparticles via Trigonella Foenum-Graecum Seed Extract for Antibacterial Response. *Pakistan Journal of Analytical & Environmental Chemistry* **19** (2), 122–127.

Khand, N. H., Solangi, A. R., Ameen, S., Fatima, A., Buledi, J. A., Mallah, A., Memon, S. Q., Sen, F., Karimi, F. & Orooji, Y. 2021 A new electrochemical method for the detection of quercetin in onion, honey and green tea using Co3O4 modified GCE. *Journal of Food Measurement and Characterization* **15** (4), 3720–3730.

Kharade Suvarta D., Nikam Gurunath H., Mane Gavade Shubhangi J., Patil Sachinkumar R. & Gaikwad Kishor V. 2020 Biogenic synthesis of cobalt nanoparticles using Hibiscus cannabinus leaf extract and their antibacterial activity. *Res J Chem Environ* **24** (5), 9–13.

Klink, M. J., Laloo, N., Leudjo Taka, A., Pakade, V. E., Monapathi, M. E. & Modise, J. S. 2022 Synthesis, characterization and antimicrobial activity of zinc oxide nanoparticles against selected waterborne bacterial and yeast pathogens. *Molecules* **27** (11), **3532**.

Koyyati, R., Kudle, K. R. & Padigya, P. R. M. 2016 Evaluation of antibacterial and cytotoxic activity of green synthesized cobalt nanoparticles using Raphanus sativus var. *longipinnatus leaf extract. International journal of pharmtech research* **9** (3), 466–472.

Kumar, A. & Schweizer, H. P. 2005 Bacterial resistance to antibiotics: Active efflux and reduced uptake. *Advanced drug delivery reviews* **57** (10), 1486–1513.

Langford, B. J., So, M., Raybardhan, S., Leung, V., Westwood, D., MacFadden, D. R., Soucy, J.-P. R. & Daneman, N. 2020 Bacterial co-infection and secondary infection in patients with COVID-19: A living rapid review and meta-analysis. *Clinical microbiology and infection* **26** (12), 1622–1629.

Lanje, A. S., Sharma, S. J., Pode, R. B. & Ningthoujam, R. S. 2010 Synthesis and optical characterization of copper oxide nanoparticles. *Adv Appl Sci Res* **1** (2), 36–40.

Lee, S. Y., Jang, H. W., Lee, H. R. & Joh, H. I. 2021 Size effect of metal-organic frameworks with iron single-atom catalysts on oxygen-reduction reactions. *Carbon Letters* **31** (6), 1349–1355.

Maruthupandy, M., Rajivgandhi, G. N., Quero, F. & Li, W.-J. 2020 Anti-quorum sensing and anti-biofilm activity of nickel oxide nanoparticles against Pseudomonas aeruginosa. *Journal of Environmental Chemical Engineering* **8** (6),104533.

Megarajan, S., Ameen, F., Singaravelu, D., Islam, M. A. & Veerappan, A. 2022 Synthesis of N-myristoyltaurine stabilized gold and silver nanoparticles: Assessment of their catalytic activity, antimicrobial effectiveness and toxicity in zebrafish. *Environmental Research* **212**, 1–9.

Memon, S. A., Hassan, D., Buledi, J. A., Solangi, A. R., Memon, S. Q. & Palabiyik, I. M. 2020 Plant material protected cobalt oxide nanoparticles: sensitive electro-catalyst for tramadol detection. *Microchemical Journal* **159**, 105480.

Nithya, C., Begum, M. F. & Pandian, S. K. 2010 Marine bacterial isolates inhibit biofilm formation and disrupt mature biofilms of Pseudomonas aeruginosa PAO1. *Applied microbiology and biotechnology* **88** (1), 341–358.

Organization, W. H. 2017 Implementation of the global action plan on antimicrobial resistance. *WHO GAP AMR Newsl* **30**, 1–4.

Parks, M. & Messmer, T. 2015 Characteristics of electronic cigarette users and their smoking cessation outcomes. *Cancer* **121**, 800.

Pena, M. M. O., Koch, K. A. & Thiele, D. J. 1998 Dynamic regulation of copper uptake and detoxification genes in Saccharomyces cerevisiae. *Molecular and cellular biology* **18** (5), 2514–2523.

Randall, C. P., Mariner, K. R., Chopra, I. & O'Neill, A. J. 2013 The target of daptomycin is absent from Escherichia coli and other gram-negative pathogens. *Antimicrobial agents and chemotherapy* **57** (1), 637–639.

Raza, M. A., Kanwal, Z., Riaz, S. & Naseem, S. 2016 Synthesis, characterization and antibacterial properties of nano-sized cobalt particles. In: *Proceedings of the 2016 World Congress on Advances in Civil, Enviromental, and Materials Research (ACEM16)*, Jeju Island, Korea,

Reddy, K. M., Feris, K., Bell, J., Wingett, D. G., Hanley, C. & Punnoose, A. 2007 Selective toxicity of zinc oxide nanoparticles to prokaryotic and eukaryotic systems. *Applied physics letters* **90** (21), **213902**.

Sagadevan, S. & Podder, J. 2015 Investigations on structural, optical, morphological and electrical properties of nickel oxide nanoparticles. *International Journal of Nanoparticles* **8** (3-4), 289–301.

Saleh, M. M., Refa't A, S., Latif, H. K. A., Abbas, H. A. & Askoura, M. 2019 Zinc oxide nanoparticles inhibits quorum sensing and virulence in Pseudomonas aeruginosa. *African health sciences* **19** (2), 2043–2055.

Shahzadi, T., Zaib, M., Riaz, T., Shehzadi, S., Abbasi, M. A. & Shahid, M. 2019 Synthesis of eco-friendly cobalt nanoparticles using Celosia argentea plant extract and their efficacy studies as antioxidant, antibacterial, hemolytic and catalytical agent. *Arabian Journal for Science and Engineering* **44**, 6435–6444.

Sharifipour, E., Shams, S., Esmkhani, M., Khodadadi, J., Fotouhi-Ardakani, R., Koohpaei, A., Doosti, Z. & Ej Golzari, S. 2020 Evaluation of bacterial co-infections of the respiratory tract in COVID-19 patients admitted to ICU. *BMC infectious diseases* **20** (1), 1–7.

Shkodenko, L., Kassirov, I. & Koshel, E. 2020 Metal oxide nanoparticles against bacterial biofilms: Perspectives and limitations. *Microorganisms* **8** (10), **1545**.

Singh, G., Joyce, E. M., Beddow, J. & Mason, T. J. 2012 Evaluation of antibacterial activity of ZnO nanoparticles coated sonochemically onto textile fabrics. *Journal of microbiology, biotechnology and food sciences* **2** (1), 106–120.

Theodora, N. A., Dominika, V. & Waturangi, D. E. 2019 Screening and quantification of anti-quorum sensing and antibiofilm activities of phyllosphere bacteria against biofilm forming bacteria. *BMC research notes* **12** (1), 1–5.

Tunio, S. A., Afreen, U., Bano, S. & Sharif, M. 2020 Evaluation of antibacterial activity of zinc oxide nanoparticles and acrylamide composite against multidrug-resistant pathogenic bacteria. *Pakistan Journal of Analytical & Environmental Chemistry* **21** (1), 125–131.

Uroz, S., Dessaux, Y. & Oger, P. 2009 Quorum sensing and quorum quenching: the yin and yang of bacterial communication. *ChemBioChem* **10** (2),205-216.

Wikler, M. A. 2006 Methods for dilution antimicrobial susceptibility tests for bacteria that grow aerobically: approved standard. *Clsi (Nccls)* **26**, M7–A7.

Yamamoto, O. 2001 Influence of particle size on the antibacterial activity of zinc oxide. *International Journal of Inorganic Materials* **3** (7), 643–646.

Yu, H. S., Li, P., Zhang, L. W., Zhu, Y. X., Al-Zahrani, F. A. & Ahmed, K. 2020 Application of optical fiber nanotechnology in power communication transmission. *Alexandria Engineering Journal* **59** (6), 5019–5030.

Zhang, Z. & Karimi-Maleh, H. 2023a In situ synthesis of label-free electrochemical aptasensor-based sandwich-like AuNPs/PPy/Ti3C2Tx for ultrasensitive detection of lead ions as hazardous pollutants in environmental fluids. *Chemosphere*, 138302. https://doi.org/10.1016/j.chemosphere.2023.138302.

Zhang, Z. X. & Karimi-Maleh, H. 2023b Label-free electrochemical aptasensor based on gold nanoparticles/titanium carbide MXene for lead detection with its reduction peak as index signal. *Advanced Composites and Hybrid Materials* **6** (2), 1–11.

Zorkipli, N. N. M., Kaus, N. H. M. & Mohamad, A. A. 2016 Synthesis of NiO nanoparticles through sol-gel method. *Procedia chemistry* **19**, 626–631.

First received 28 February 2023; accepted in revised form 3 May 2023. Available online 15 May 2023